Available online at www.sciencedirect.com

ScienceDirect

Procedia CIRP 123 (2024) 238–243

www.elsevier.com/locate/procedia

7th CIRP Conference on Surface Integrity

Development of an Analytical Model for Correlation with Workpiece Roughness in Stream Finishing using a LiDar Sensor

Florian Sauer[a*], Patrick Neuenfeldt[b], Germán González[a], Volker Schulze[a]

[a] wbk Institute of Production Science of Karlsuhe Institute of Technology (KIT), Kaiserstr. 12, 76131 Karlsruhe, Germany
[b] SADEN GmbH, Amalienstraße 75, 76133 Karlsruhe, Germany

* Corresponding author. Tel.: +49 721 608 44288; fax: +49 721 608-45005. *E-mail address:* Florian.Sauer@kit.edu

Abstract

The stream finishing process is often used for smoothing metal surfaces. It is commonly utilized in the high-precision finishing process of high-performance components, which shall not present any roughness gradient along the surface to avoid degrading its mechanical properties. Although many research works have studied the stream finishing process using experimental and simulative approaches, predicting the generated surface quality remains a challenge. In this work, LiDAR-sensor measurements have been conducted for an in-process analysis and real-time surface roughness prediction. The presented analytical approach obtains the process intensities resulting from the local forces. The resulting intensities show a linear correlation with the surface roughness enabling a forecast of the process-related gradient along the surface of the part during the stream finishing process, which allows the optimization of the process parameters and improvement of the surface quality.

Keywords: LiDar; Stream Finishing; Roughness Correlation

1. Introduction

Finishing processes are becoming increasingly important in production engineering, with mass finishing processes standing out for improving surface quality and functionality [1]. In particular, they offer advantages in terms of precision, efficiency and reproducibility, whereby optimised tribological properties and increased service lives of components can be achieved [2]. The stream finishing process is a high intensity mass finishing process with a guided workpiece and thus a defined position in the media flow. This enables precise machining of complex and filigree components, such as those used in aerospace and medical technology [3]. In the state of the art extensive experimental work can be found on the analysis of the grinding speeds and pressures that occur as well as on the formation of the material removal [4] [5]. Moreover, fundamental works on the effects of the material change in perspective of compressive residual stresses, hardness and surface topography were already conducted [7]. By means of numerical simulations based on the discrete element method (DEM) and computer fluid dynamics (CFD), it is possible to calculate the complex three-dimensional flow field and determine relevant variables in the media as well as on the workpiece surface [6] [8] [9]. Regarding real-time capability, numerical simulations are not suitable, due to long calculation times. In the related process of vibration finishing, additional approaches have been implemented to measure the velocity fields of the surface medium using PIV, which is an important input variable for the generated abrasion [10], which has already been analyzed on the basis of abrasive finishing theory[11]. However, the process design of stream finishing requires a high degree of experience and fast methods for in-process analysis do not yet exist.

In this paper, a completely new approach for the analytical calculation of process intensities and derived roughness development is presented based on LIDAR and roughness measurements.This work aims to predict the intensity of the stream finishing process in terms of media distribution, based

10.1016/j.procir.2024.05.043

on easy-to-measure physical process parameters. For this purpose, a simplified analytical model was developed and the calculated intensities were compared with experimental data. The influence of the wall distance was investigated and set in correlation with the measured surface roughness.

2. Experimental Setup

The tests were carried out using a SF740 stream finishing machine (Otec Präzisionsfinish GmbH) with a drum diameter of 780 mm. The media used was alumina based KXMA 16 granular material with a particle size between 0.5 and 2.25 mm and a randomly, edgy shape. To prevent corrosion of the workpieces while processing and to clean the media a continuous compound flow rate of 105 l/h was used. Figure 1a illustrates the basic setup of the stream finishing tests carried out and Table 1 shows the overview of the parameter used. During the tests, the rotational speed of the drum n_d = -75 min^{-1}, of the workpiece n_w = 50 min^{-1} and the distance between the workpiece and the drum bottom d_b = 50 mm were kept constant. In order to investigate the intensity of the process as a function of the wall distance, the wall distances were varied in discrete intervals according to Table 1. Furthermore, for the investigation of the intensity over time, the surface of the specimen was measured in discrete time steps according to Table 1.

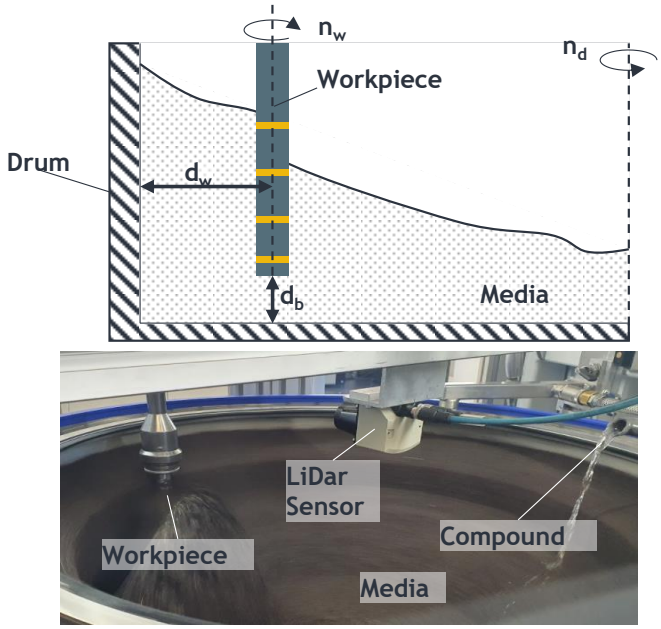

Figure 1a): Schematic drawing of the stream finishing process b) Photograph of the test setup

The media distribution is required as an input variable for the analytical calculation of the abrasion characteristics as a function of the position of the workpiece. To provide the average boundary contour (ABC) for the analytical calculation of the intensity, the media distribution was measured and digitized with a LiDar sensor of the type SICK TIM561-2050101. The LiDar Sensor was mounted on the rotational axis of the Drum with a scanning frequency set to 15 Hz, resulting in a reaction time of 67 ms. Particular care was taken to ensure that the media wall was stationary. To ensure that the media wall is stationary, the process was kept stable for 2 minutes.

In order to ensure the same initial surface characteristics for each test, the specimens were machined out of AISI4140 before the tests by longitudinal turning with the parameters *vc* = 70 m/min, feed rate 0.125 mm/rev and *ap* = 1 mm, with flood cooling. A new specimen was used for each series of tests.

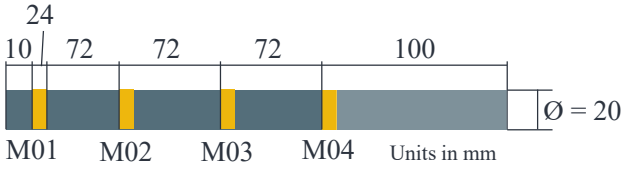

Figure 2: Measurement Position

To calculate the removal rate at the individual positions in the drum, the workpieces were measured by confocal microscopy (Nanofocus µSurf Custom) before the tests and after, at the specified time steps at the locations shown in Figure 2. In this case, an objective with a magnitude of 20, a numerical aperture of 0.4 and a resolution in the height direction of 6 nm was used. The resulting measurement field size was 1.6 to 1.6 mm. For statistical validation, all test points were repeated three times. For post-processing of the confocal measurements a cut-off wavelength of 0.75 mm and a gaussian filter according to ISO 16610-61 was utilized. The determined values of the roughness parameter Sa and the isotropy Str represent the values for the analytical correlation with the ABC.

Table 1: Variation of wall distance and used time steps

Measurment No.	1	2	3	4	5
d_w [mm]	55	89	126	149	---
Time [s]	30	60	120	240	480
Process-parameter	n_w	n_d	d_b	drum diameter	compound flow rate
	50 min^{-1}	-75 min^{-1}	50 mm	780 mm	105 l/h

3. Analytical Modelling

The analytical model developed is based on the measured media distribution with the LiDar sensor in the first step. Subsequently, the media distribution is specified as a boundary contour and inserted into the model. In the second step, the area below the curve is subdivided into a discrete mesh in axial and radial direction. The accuracy of the analytical model results from the discretization by *x*+*n* and *y*+*n*, since the forces acting at the nodes are calculated during the analysis. In the third step of the calculation, the partial forces acting on the particles in x and y direction are calculated. For the calculation of the axial forces affecting the particles, Pascal's law is used, which results in equation 1:

$$I_a = m_a \cdot g \qquad \text{with:} \qquad m_a = \cancel{\rho} \cdot \cancel{A} \cdot h_{(y)} \qquad (1)$$

Considering a 1D point in the analytical model, the term m can be assumed to be massless as well as area-less. This

shortens the term to the assumption of the resulting particle height above the point under investigation and leads to the assumption m=h(y).

By this assumption the acting static pressure can be calculated for each point of the selected mesh multiplied by the acting gravitational force.Similarly, the radial force acting on the particles can be calculated by the approaches given in equation 2

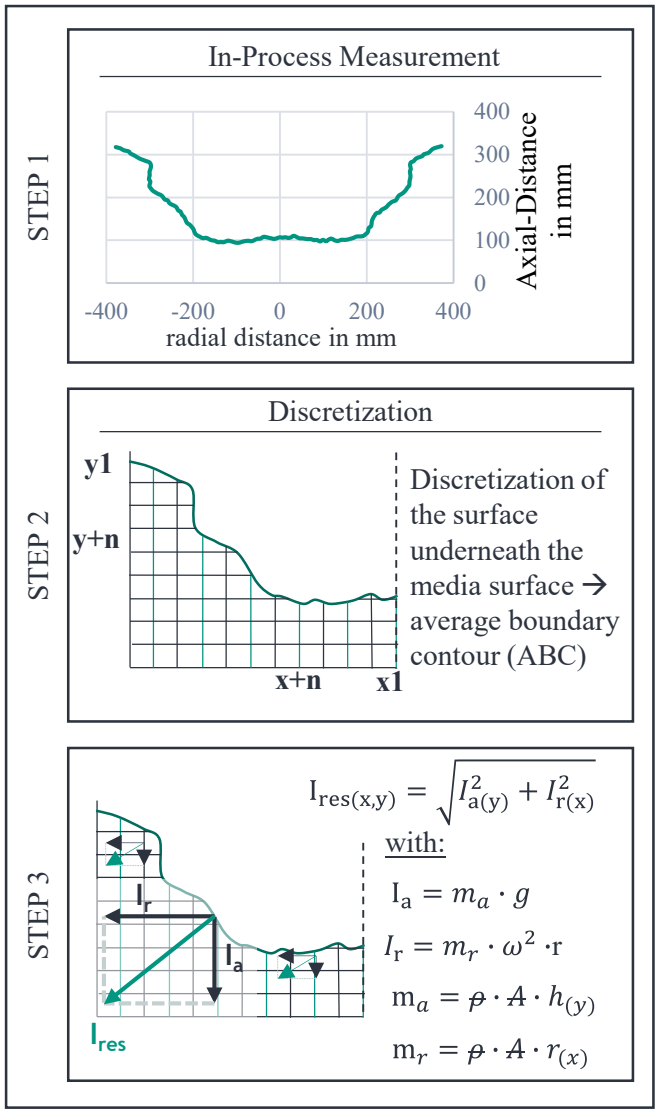

Figure 3 Analytical approach of calculating the intensity

$$I_r = m_r \cdot \omega^2 \cdot r \qquad \text{with:} \qquad m_r = \rho \cdot A \cdot r_{(x)} \qquad (2)$$

The approach according to equation 1 of the mass- and area-less consideration of the discretization is also applied in this case. Similarly, the forces acting on the particles are included in the force calculation as a function of the position considered and thus the acting horizontal particle pressure pillar. By the calculation of the individual partial component of the acting force on the locally considered particles given by the ABC, the resulting mass free forces on the discrete points can be determined via formula 3. The resulting terms are then used to calculate the mass and area free intensity of the process under investigation.

$$I_{res(x,y)} = \sqrt{I_{a(y)}^2 + I_{r(x)}^2} \qquad (3)$$

4. Results and Discussion

4.1. Experimental results

The measured mean arithmetic heights Sa are shown in Figure 4a for the different investigated wall distances according to Table 1. The roughness are shown over the positions along the workpiece axis measured according to Figure 2 for the different machining times according to Table 1. Furthermore, Figure 4b shows the measured media distribution of the different wall distances.

For all investigated specimens the initial roughness at time t=0 is constant over the measuring points and prior to machining on the same level which is between Sa 1.13 µm and 1.31 µm for the mean values. For the investigated wall distances 126 mm and 149 mm, no measured values were acquired for the fourth measuring point (uppermost), since this could not be reached during the tests due to the resulting media distribution as shown in Figure 4b. The following applies to all measured values: the longer the processing time of the sample, the lower the scatter of the measured values, which indicates a stable and uniform removal process. Furthermore, the roughness depth curves can be used to analyze the removal rate as a function of the bottom distance on the basis of the measured samples and their measuring point. In the following, the individual wall distances will be considered individually and compared with each other.

For the wall distance WD 55mm, it can be determined for the complete machining time of 480s that the minimum achievable roughness for the measuring points M01 and M02 of Sa 0.16 µm is reached, which means that further machining at these points does not lead to any improvement in the roughness. However, it can also be seen that there is a roughness distribution along the workpiece axis which is due to the granulate distribution and refers to the observed gradient. This gradient appears over the different processing times. Figure 4 further shows that the removal rate for measuring point M04, which is the furthest from the bottom of the bowl, is the lowest. Up to the processing time of t = 120 s, a linear progression of the measured roughness Sa can be determined, which is no longer reflected in the further time steps. However, the linear roughness gradient is still valid for the measuring points M01 to M03. This behavior of the roughness gradient in the axial direction is even more clearly visible at a wall distance of 89 mm. Furthermore, the measured values of the wall distance WD 89mm for the fourth measuring point do not show any significant removal over the complete machining time.

This behavior is plausible, since this measuring point is only marginally processed by the granulate, as shown in Figure 4b. However, for the first measuring point a comparable roughness of 0.17 µm is achieved as for wall distance 55 mm after 480 s processing. For the measuring positions M02 and M03, however, a greater depth gradient of the roughness can be observed in comparison. Thus, the influence of the wall distance can already be qualitatively shown in the following analysis.

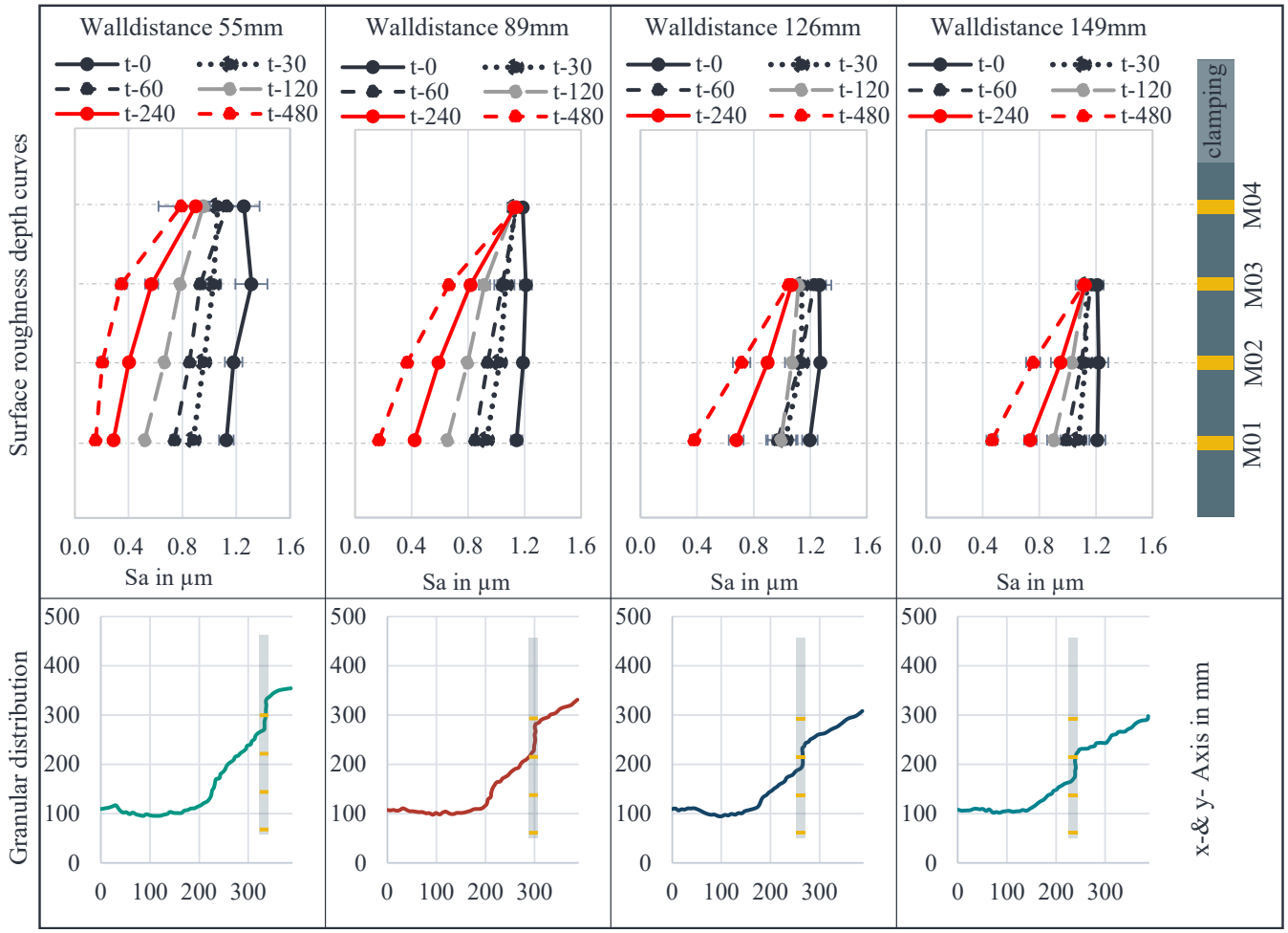

Figure 4 a) Measured roughness values Sa for the investigated different wall distances and processing time b) Granulate distribution in dependence of the wall distance.

Comparing the two wall spacings 126 mm and 149 mm to each other, the samples with the wall spacing 126 mm have a roughness Sa of 0.38 µm after 480s processing time and the samples with the WD 149mm have a roughness of 0.47 µm. Roughness is also linear along the axes of the workpiece. A comparison of all the measured values shows that the material removal rate is in direct proportion to the distance from the wall. Furthermore, a clear dependence of the material removal ratio on the height of the media distribution can be identified. Thus, it may be concluded that the media distribution, which is determined by the initial filling level and diameter of the drum, has a direct influence on the removal behavior.

Further, the intensity of the process can be related to the circumferential speed as well as the filling level of the granules.

4.2. Analytical Calculation and validation

The calculated intensities of the process according to the procedure described in chapter *"Analytical Modelling"* are shown in Figure 5. The off-color diagrams show the measured granular distribution through the represented workpieces as in Figure 4b for the examined wall distances and thus represent the boundary of the calculation. Moreover, the resulting intensity due to the different distribution of the particles is shown in the diagrams. Regardless of the wall distance investigated, the greatest mass and surface intensity is found on the outermost diameter and on the bottom of the drum with a maximum value of 16.3 mm^2/s^2. This result was to be expected with the chosen analytical approach, since the largest hydrostatic force and the largest particle volume with the centrifugal force act in this area. The gradient of the intensity in the radial dimension corresponds well to the granular distribution and the physical effect. The larger the selected wall distance, the lower the intensity and thus the lower the ablation volume. The gradient in the axial direction can also be determined: the greater the distance to the bottom, the lower the removal rate. These two findings explain the measured roughness depth curves as a function of the selected wall distance in Figure 4a of the measured specimens.

Furthermore, with regard to the intensity of the process, the position of the workpiece and the resulting media distribution do not have a significant influence, but remain qualitatively the same for high intensities in the left area of the drum. Thus, the large removal volume, the resulting gradient distribution and the smoothing of the surface at a small wall distance with high intensity caused by the gravitational and centrifugal forces can be justified. However, this assumption is not valid for lower intensities, so in comparison between wall distance 55mm and wall distance 149mm the influence of the granule distribution by the positioned workpiece on the intensity on the left side of

$$r = \frac{\sum(x-\bar{x})(y-\bar{y})}{\sqrt{\sum(x-\bar{x})^2 \sum(y-\bar{y})^2}} \qquad (4)$$

the specimen is observed. This is due to the effect of the centrifugal particle pillar and represents a plausible result. Using the roughness gradient determined after t = 480 s according to Figure 4a and the gradient of the existing intensities from Figure 5, the dependence of these two values on each other is presented in Figure 6. The figure shows where the intensity of the process is highest, the resulting surface roughness is also lowest. Furthermore, it appears that the determined roughness correlate inversely to the calculated intensities.

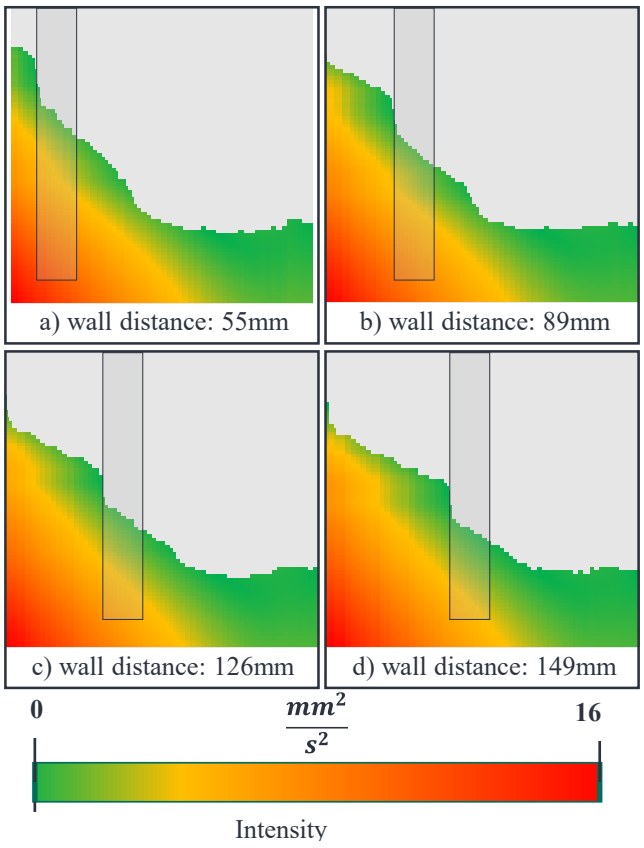

Figure 5 Calculated intensity as a function of the workpiece wall distance

The Pearson's approach according to formula 4 was chosen to verify the inverse correlation, which gives the relationships between the intensity and roughness gradients.
In Table 2, the surface roughness at the four measuring points of the workpiece for the processing time of t=480s and the intensities calculated from the analytical model at the measuring points is given for the different wall distances. The Pearson correlation coefficient was determined from these values according to formula 4. For the wall distances WD126 mm and WD149 mm, a coefficient of almost -1 can be determined, which corresponds to a negative correlation between the intensity of the process and the resulting roughness gradient. For the wall distances WD55 mm and WD89 mm the determined Pearson correlation coefficient deviates slightly from -1. For WD89 mm this is approximately -0.96 and for the wall distance WD55 mm approximately -0.88. The deviation from an ideal correlation at a smaller wall distance can be explained by the fact that, as described in *"Experimental results"*, the roughness limit of the processed specimens has already been reached.

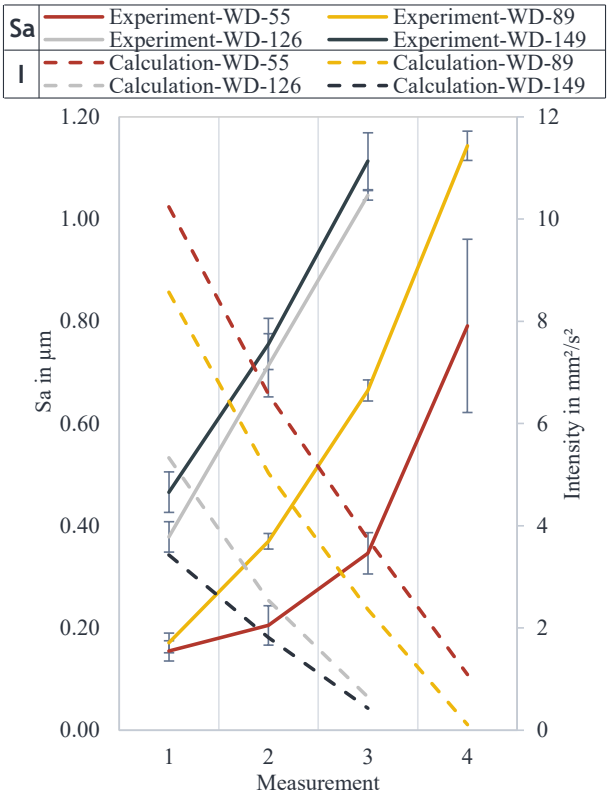

Figure 6 Comparison of intensity vs. roughness after 480s processing time for the investigated wall distances

This means that the surface roughness is not expected to improve with longer processing times. Instead, a longer processing time will change the geometry and thus the diameter of the workpiece. These effects cannot be predicted and mapped with the analytical model developed.

Table 2 Intensity values and roughness values along the measured axial measuring areas and determined pearson corelation coefficients for t=480s

	WA55		WA89		WA126		WA149	
Measuring point	Intensity	Roughness Sa	Intensity	Roughness Sa	Intensity	Roughness Sa	Intensity	Roughness Sa
Unit	[mm²/s²]	[µm]	[mm²/s²]	[µm]	[mm²/s²]	[µm]	[mm²/s²]	[µm]
1	10.24	0.16	8.57	0.17	5.33	0.38	3.43	0.47
2	6.57	0.21	5.03	0.37	2.54	0.71	1.81	0.76
3	3.74	0.35	2.36	0.66	0.65	1.05	0.43	1.11
4	1.09	0.79	0.11	1.14	---	---	---	---
Pearson	-0.8844		-0.9569		-0.9942		-0.9943	

To illustrate this restriction in the analytical model in detail, Figure 7 shows the roughness distribution of the samples with a wall spacing of 55 mm after a processing time of 120 s and 240 s as well as the determined intensity. With the help of these values, the Pearson correlation can be determined for the discrete time steps in Table 3. The negative correlation of -0.95 for the processing time of 240s for the wall distance of 55mm is comparable to the correlation of the values determined for the wall distance of 89mm.

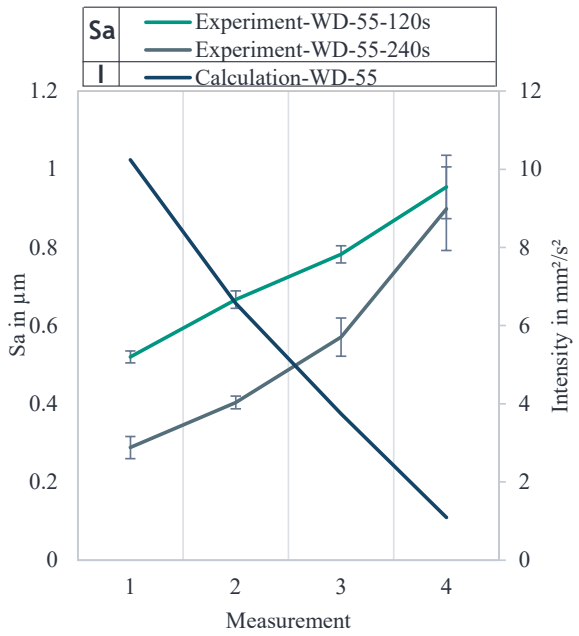

Figure 7 Roughness gradient for WD55mm at 120s and 240s in comparison with calculated intensity

The intensity and the roughness gradient at 120s for WD 55mm show an almost perfect correlation of the two observed curves. This indicates that the geometry of the samples has already changed before the processing time of 240s.

Thus, the limits of the analytical model become evident, meaning this analytical model can determine the roughness gradients along the workpiece axis in dependence of the wall distance with a high correlation to the measured values as long as there is no geometric change of the specimens.

Table 3 roughness values for WD-55mm for process time 120s and 240s and the resulting Pearson coefficient

	WA55		
Measuring point	Intensity	Roughness Sa -120s	Roughness Sa -240s
Unit	[mm2/s2]	µm	µm
1	10.24	0.52	0.29
2	6.57	0.67	0.40
3	3.74	0.78	0.57
4	1.09	0.95	0.90
Pearson		-0.9925	-0.9522

5. Conclusion and Outlook

The introduced method represents a simple and fast method to numerically determine the existing surface roughness gradient during stream finishing by means of an easy to measure granulate distribution. The model has the following properties:

- Determination of the influence of the wall and bottom distance of the specimens on the development of the settling roughness gradient.
- Method is valid as long as there is no geometrical change of the specimens.
- The calculated intensity in the process correlates inversely to the roughness gradient along the workpiece axis.
- Currently only tested for simple geometries

The model is to be further developed in the near future in order to be able to predict the roughness as a function of the intensity. Furthermore, the time dependence of the evolution of the roughness shall be predicted with this model. It is necessary to confirm this analytical model for more complex contours as well as different granulate.

This will eliminate the need for complex 3D simulations of the entire process for simple geometries and allow the roughnesses to be predicted precisely in the process.

Acknowledgements

All authors thank the German Federation of Industrial Research Association (AiF) for the financial support and the partner OTEC Präzisionsfinish GmbH for the support and provision of the stream finishing machine.

References

[1] Hashimoto, F.; Yamaguchi, H.; Krajnik, P.; Wegener, K.; Chaudhari, R.; Hoffmeister, H.-W. & Kuster, F. (2016), „Abrasive fine-finishing technology“, CIRP Annals - Manufacturing Technology (65), S. 597–620.

[2] Baghbanan, M. R.; Yabuki, A.; Timsit, R. S. & Spelt, J. K. (2003), „Tribological behavior of aluminum alloys in a vibratory finishing process“, Wear, 255 (7-12), S. 1369–1379.

[3] Vijayaraghavan, V. & Castagne, S. (2018), „Measurement of surface characteris tics of Ti6Al4V aerospace engineering components in mass finishing process“, Measurement, 115, S. 279–287.

[4] Brocker, R. (2015), Relativgeschwindigkeiten und Kontaktkräfte beim ungeführten Vibrationsgleitschleifen, Apprimus Verlag, Aachen. ISBN: 978-9-86359-334-6.

[5] Cariapa, V.; Park, H.; Kim, J.; Cheng, C. & Evaristo, A. (2008), „Development of a metal removal model using spherical ceramic media in a centrifugal disk mass fin ishing machine“, The International Journal of Advanced Manufacturing Technology (39), S. 92–106.

[6] Zanger, F.; Kacaras, A.; Neuenfeldt, P. & Schulze, V. (2019), „Optimization of the stream finishing process for mechanical surface treatment by numerical and ex perimental process analysis“, CIRP Annals - Manufacturing Technology (68), S. 373–376.

[7] Schulze, V.; Gibmeier, J. & Kacaras, A. (2016), „Qualification of the stream finishing process for surface modification“, CIRP Annals - Manufacturing Technology (66), S. 523–526.

[8] Makiuchi Y., Hashimoto F., Beaucamp A. (2019), “Model of material removal in vibratory finishing, based on Preston’s law and discrete element method”, CIRP Annals - Manufacturing Technology (68), S. 365–368.

[9] Mullany B., Shahinian H., Navare J., Azimi F., Fleischhauer E., Tkacik P., Keanini R. (2017),” The application of computational fluid dynamics to vibratory finishing processes”, CIRP Annals - Manufacturing Technology (66), S. 309–3312.

[10] Fleischhauer E.,Azimi F., Tkacik P.,Keanini R.,Mullany B., “Application of particle image velocimetry (PIV) to vibrational finishing”, Journal of Materials Processing Technology 229 (2016) 322–328.

[11] Hashimoto F., Johnson S. F., Chaudhari R.G.,” Modeling of material removal mechanism in vibratory finishing process”, “, CIRP Annals - Manufacturing Technology (65), S. 325–328.